Journal of Particle Science and Technology 7 (2) (2021) 119-130

Ministry of Science, Research & Technology
Iranian Research Organization for Science and Technology

Journal of PARTICLE Science & Technology

JPSIT

https://jpst.irost.ir

Research paper

Investigation of phosphate adsorption from aqueous media using synthetic mordenite and modified natural clinoptilolite zeolite adsorbents: characteristics, kinetics, and isotherms

Hossein Pazoki, Mansoor Anbia*

Research Laboratory of Nanoporous Materials, Department of Chemistry, Iran University of Science and Technology, Tehran, Iran

HIGHLIGHTS

- Removal of phosphate from aqueous solution by synthetic mordenite and modified clinoptilolite zeolite has been investigated.
- The maximum adsorption capacities by synthetic mordenite and modified clinoptilolite zeolite were 23.06 and 17.9 mg.g^{-1} for phosphate ions.
- The results confirm the efficiency of adsorbents for reduction of phosphate from aqueous solution.
- The results of the present study indicate that sorption capacity of mordenite is higher than MnO_2-clino.

GRAPHICAL ABSTRACT

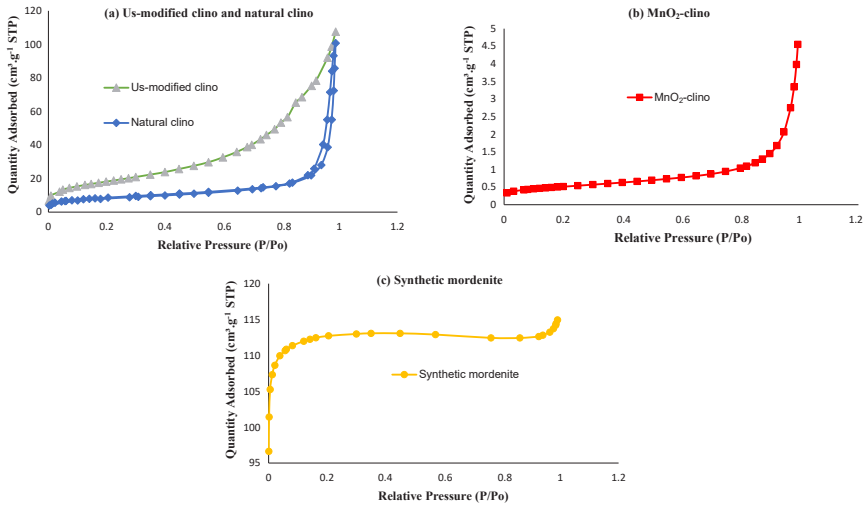

ARTICLE INFO

Article history:

Received 1 September 2021
Revised 03 June 2022
Accepted 08 June 2022

Keywords:

Adsorbent
Modification
Removal
Sorption capacity
Solvothermal

ABSTRACT

This study investigates phosphate removal from aqueous solution by synthetic mordenite and modified clinoptilolite zeolite. The mordenite zeolite was synthesized using the solvothermal method, and natural clinoptilolite zeolite was modified by ultrasound energy and manganese dioxide. The adsorbents were characterized by utilizing X-ray diffraction (XRD), Fourier transform infrared (FT-IR), Scanning electron microscope (SEM) images, energy dispersive X-ray analysis (EDXA), and the Brunauer-Emmet-Teller (BET) method. This study investigated the adsorption behavior of the two adsorbents, including the influence of solid/liquid ratio, contact time, initial concertation, and modification of the adsorption process, adsorption kinetics, and isotherms. The maximum phosphate adsorption capacity of the modified synthetic mordenite and the modified clinoptilolite are 23.06 and 17.9 mg.g^{-1}, respectively, which is higher than the values reported in other studies. The present study shows that the amount of adsorption of modified synthetic mordenite for phosphate removal is higher than the modified clinoptilolite zeolite. The kinetics study shows that the pseudo-second-order kinetic equation better describes the adsorbents' adsorption behavior. The isotherms study suggests that the adsorption process of synthetic mordenite and modified clinoptilolite zeolite follow the Langmuir and Freundlich models, respectively.

* *Corresponding author: Tel.: +9821-77240516 ; Fax: +9821-77491204 ; E-mail address: anbia@iust.ac.ir*
DOI: 10.22104/JPST.2022.5172.1192

1. Introduction

Water, food, and air are necessities for humans, but water is the most important. Most water pollution is caused by lagged agriculture, industrial development, and urbanization [1]. Today, eutrophication is a serious issue in water quality management; it causes plants and algae to grow quickly, destroying aquatic life and accelerating water scarcity [2]. Many human cancers are caused by noxious toxins produced during the eutrophication process, collected in aquatic animals, and then transmitted to humans [3]. Phosphate (P) is an important nutritional composition, but excessive phosphate causes acceleration of eutrophication, dissolved oxygen depletion, and death of aquatic organisms [4]. Therefore, too much phosphate can lead to serious environmental hazards and risks to human health [5]. The major limiting factor for eutrophication is phosphorus released into the environment by agriculture, food wastes, urban run-off, animal wastes, human sewage, industry, and detergents [6,7]. Therefore, water quality management must control the amount and reduce the harmful effects of phosphorus [8]. Various methods of chemical and biological technologies to remove phosphate have been widely investigated in recent years [9-13].

The chemical methods include adsorption, ion exchange, and precipitation. Common precipitants such as lime, aluminum sulfate, and ferric chloride are used for precipitation [9]. However, several disadvantages of the precipitation methods, such as the cost of metal salts and the production and dewatering of sludge, prevent its widespread use [11]. Biological technology removes phosphate with phosphate-accumulating organisms that reduce the phosphate in the cyclic anaerobic and aerobic sequence. The biological techniques have convenient features that include producing less sludge and being economically viable, but factors such as the composition, temperature, and pH in wastewater affect the efficiency of the phosphate removal [13]. The adsorption process is the most effective and widely used application in the sewage treatment process due to its advantageous properties, such as non-toxicity, easy design, good effectiveness, applicability in a wide range of concentrations, ability to recover the adsorbent, and availability of a wide range of adsorbents [14,15].

Many adsorbents have been studied to reduce phosphorus in the aquatic environment. In recent years, zeolites have been recognized as a good choice for the adsorption process because of their special properties, such as the proper surface area, high hydrothermal and thermal stabilities, proper adsorption capacity, and low cost. Synthetic and natural zeolites are microporous crystalline aluminosilicate minerals that have three-dimensional networks consisting of $[SiO_4]^{4+}$ and $[AlO_4]^{4-}$ [16-19]. The low adsorption capacity and removal efficiency are disadvantages of using natural zeolite in the adsorption process. So, the modification of natural zeolite is necessary for using the compounds in industrial applications. Natural zeolite can be modified using acid, alkali, surfactant, or salt [20,21], microwave irradiation [22], sonification, and heat treatment [23] methods to improve adsorption capacity and removal efficiency. In addition to natural zeolites, high-quality zeolites are synthesized using a wide range of silicon and aluminum sources by various methods. With their high sorption capacity, synthetic zeolites are preferred to natural zeolites [24-28]. There are several important parameters for synthesis, such as temperature, time, and pH [29].

The current work aims to investigate modified natural clinoptilolite and synthetic mordenite zeolite for phosphate removal. First, the mordenite zeolite was synthesized under solvothermal conditions without introducing any organic compounds. Then, the natural clinoptilolite zeolite was modified by ultrasound energy and manganese dioxide. Next, these adsorbents were characterized by XRD, SEM, EDXA, FT-IR, and BET techniques. Afterward, the phosphate adsorption of the modified natural clinoptilolite and synthetic mordenite zeolite were examined by varying factors such as solution time, adsorbent dosage, and phosphate concentration. Finally, the adsorbents' kinetics and isotherms of phosphate adsorption were studied.

2. Materials and methods

2.1. Materials

Natural clinoptilolite was purchased from the Semnan Negin Powder Company, Iran. Sodium hydroxide (NaOH) (Merck, 99%), sodium aluminate ($NaAlO_2$) (Merck, 99%), manganese (II) nitrate tetrahydrate ($Mn(NO_3)_2{\cdot}4H_2O$) (Merck, 99%), potassium permanganate ($KMnO_4$) (Merck, 99%), and colloidal silica sol (Ludox SM, 30% SiO_2, 70% H_2O, <1% Na_2O) with sodium stabilizer were obtained and used with-out purification.

2.2. Modification of natural clinoptilolite zeolite

In the first step, an alkali solution was prepared by dissolving 1.2 g of NaOH in 30 ml of deionized water. 2 g of natural clinoptilolite was added to 30 ml of the prepared alkali solution. Then, the mixture was agitated using an ultrasonic processor with a standard probe (i.e., 13 mm diameter tip) under atmospheric pressure at 60 °C for 2 h. The ultrasound process produces acoustic waves at a frequency of 20 kHz, and the ultrasound wave was 150W. The sorbent was denoted as Us-clino. Next, the modified zeolites were filtered, washed thoroughly with deionized water, dried overnight at 100 (±1) °C using an electric oven, and then characterized by different instrumental techniques [30].

In the second step, natural clinoptilolite zeolite was modified with MnO_2 in three stages:

- The mixture of 10 g clinoptilolite and 14 ml of 1 M $Mn(NO_3)_2$ was stirred for 3h at 20 °C.
- The Mn^{2+} ion into clinoptilolite was treated with a 0.5% KMnO4 solution for 3h at 20 ± 1 °C (solid/liquid ratio of 1:10).
- The product was recovered by filtration, washed with distilled water, and dried at 80 °C for 8 h. The modified clinoptilolite was denoted as MnO_2-clino.

2.3. Synthesis of mordenite zeolite

To synthesize mordenite, 3.73 g of sodium hydroxide was first dissolved in 70 ml of distilled water. After it was completely dissolved, 1.92 g of sodium aluminate was added to the solution. Then, the solution was stirred at 25 °C at 400 (rpm) for 1 h. Next, in another beaker, 50 ml colloidal silica was blended with 28 ml distilled water. Then, this solution was slowly added drop-wise to the first solution. The solution was then stirred at 25 °C for several minutes, which resulted in a clear homogenous solution. Next, the resultant mixture was transferred to the stainless-steel autoclave, and the temperature was set at 170 °C for 24 h. Finally, the solution was filtered and washed several times with distilled water until the pH decreased to 7-8 and dried at 90 °C for 5 h.

2.4. Characterization

A variety of conventional techniques were used for the characterization of the zeolites. X-ray diffraction was accomplished to characterize the synthesized crystalline zeolite. The zeolite patterns were obtained using a Philips 1830 diffractometer with Cu-Kα radiation, operated at 40 kV, 20 mA. The nitrogen adsorption characteristics, including the pore volume, the pore size diameter, and surface area of the surface of the adsorbent, were obtained with a micromeritics model ASAP 2020 analyzer. The Fourier transform infrared spectrum of the adsorbent was recorded at room temperature on a DIGILAB FTS 7000 spectrometer equipped with an attenuated total reflection (ATR) cell. The crystal morphology of adsorbents was investigated by a PHILIPS XL30 scanning electron microscope. In addition, an energy dispersive spectrometer (EDX, VEGA3 TESCAN) attached to SEM determined the chemical compositions of the samples.

2.5. Phosphate adsorption experiments

Phosphate adsorption was studied at 25 °C using the batch method with different initial concentrations (between 25 and 100 $mg.L^{-1}$) of the synthetic phosphate solution prepared by dissolving potassium dihydrogen phosphate (KH_2PO_4) in deionized water. To achieve equilibrium, the mixture of adsorbent and phosphate solution was constantly stirred at a rotating speed of 150 rpm at a constant temperature. The residual phosphate concentration samples were measured using a UV spectrophotometer (UV mini 1240 Shimadzu). The kinetics of phosphate sorption on adsorbents were studied at an initial phosphate concentration of 50 $mg.L^{-1}$. The kinetic studies were carried out in a 50 ml solution at pH 7 and 25 °C. Also, the equilibrium adsorption capacity (q_e, $mg.g^{-1}$), the adsorption capacity at different times t (q_t, $mg.g^{-1}$), and the percentage of phosphate adsorption ($R\%$) were calculated as follows:

$$q_e = (C_0 - C_e)\, V/W \quad (1)$$

$$q_t = (C_0 - C_t)\, V/W \quad (2)$$

$$R\% = (C_0 - C_e)/C_e \quad (3)$$

where C_0 is the initial concentration of phosphate ions ($mg.L^{-1}$), C_e is the final concentration of phosphate ions ($mg.L^{-1}$), C_t is the concentration of phosphate ions at time t ($mg.L^{-1}$), V is the volume of the aqueous (L), and W is the weight of the adsorbents (g).

3. Results and discussion

3.1. N_2 adsorption-desorption analysis

The specific surface area and pore diameter of modified natural clinoptilolite and synthetic mordenite zeolite was determined by N_2 adsorption-desorption isotherms. The N_2 adsorption-desorption isotherm results are shown in Fig. 1. The experiments clearly reveal that the surface area of the modified clino was changed compared with natural clino, which enhanced the adsorption properties of the modified clino. However, there are more reactant sites in the modified clino because the ultrasound and MnO_2 modification caused the clino's surface area with

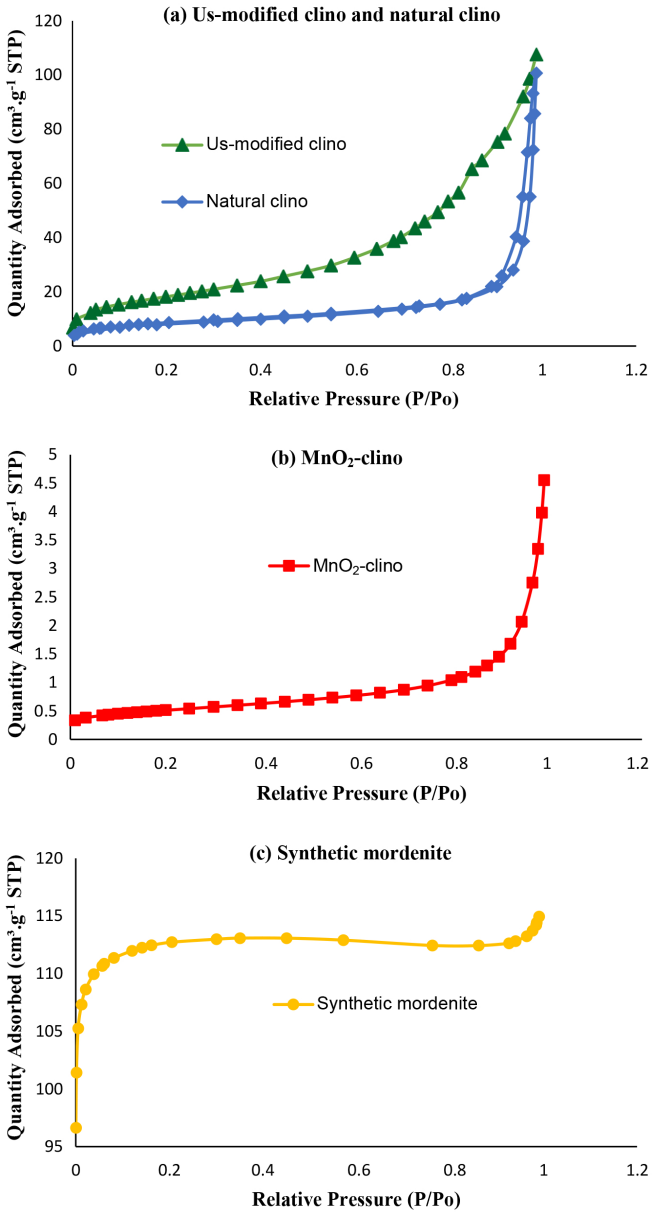

Fig. 1. Nitrogen adsorption and desorption isotherms of (a) us-modified and natural clino, (b) MnO_2-clino, and (c) synthetic mordenite.

Table 1. Textural properties determined from nitrogen adsorption–desorption experiments..

Sample	S_{BET} ($m^2.g^{-1}$)	Pore volume ($cm^3.g^{-1}$)	Pore diameter (nm)
Natural clinoptilolite	24.43	0.0637	10.09
US-modified clino	66.33	0.1599	9.82
MnO_2-clino	40.316	0.095	9.31
Synthetic mordenite	344	0.1766	2.22

66.33 and 40.316 $m^2.g^{-1}$, respectively, to be higher than the natural clino (24.43 $m^2.g^{-1}$) as seen in Table 1. Also, the isotherm of the synthetic mordenite confirmed that the compound is microporous. As the results show, the BET surface area and pore volumes are 456.59 and 104.09 $cm^3.g^{-1}$, respectively. The structural properties of the adsorbents are summarized in Table 1.

3.2. FT-IR spectra analysis

The FT-IR spectrum of the zeolites is shown in Fig. 2. The band at about 470 cm^{-1}, which is in the spectrum of the clinoptilolite, is related to T–O bending. A sharp, high-intensity peak in the range of 1052-1200 cm^{-1} is related to the Si–O–Si(Al) asymmetric stretching vibration. The spectrum showed a band at about 792 cm^{-1} related to symmetric stretching of the Si–O–Si(Al). The existence of the H–O bond in the structure of the compound can be seen at 1637 and 3622 cm^{-1}, which are related to bending vibration and stretching vibration of the O–H band of silanol groups, respectively [31].

3.3. XRD patterns of adsorbent

The characterization of crystalline modified clinoptilolite and mordenite zeolite was determined by

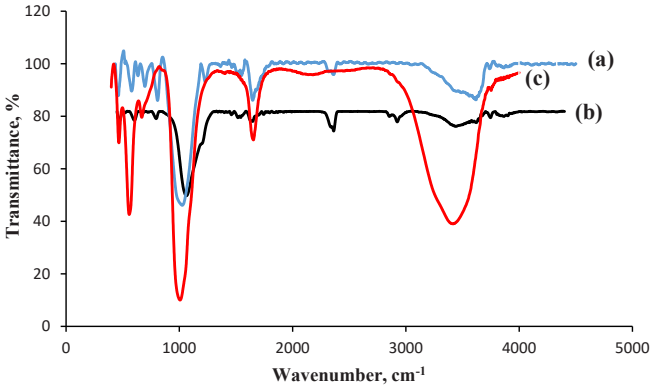

Fig. 2. FT-IR spectra of (a) Us-modified clino, (b) MnO_2-clino, and (c) Synthetic mordenite.

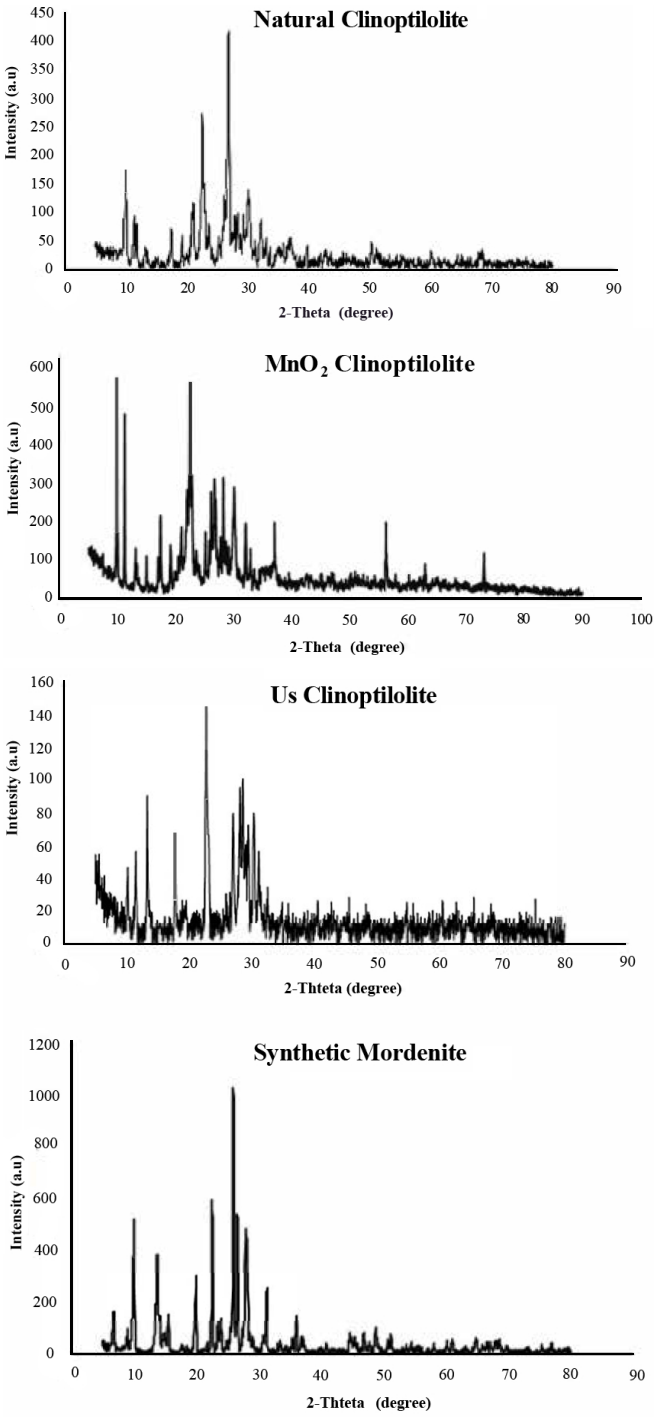

Fig. 3. XRD patterns of natural clino, us-clino, MnO_2-clino, and synthetic mordenite.

X-ray diffraction (XRD) and is shown in Fig. 3. The location of peaks observed at 2θ = 10, 20, 22, 26, 30, and 32 are similar to clinoptilolite zeolite [32]. The intensity of the modified zeolite is lower than unmodified zeolite because the ultrasonic processor decreases the crystallinity, elution of exchange cations, and aluminum of the zeolite [30]. The crystalline character of MnO_2-clino was exposed by the characteristic diffraction peaks at 2θ = 28, 36, 56, and 73, which corresponds to MnO_2 [33]. The XRD spectrum of the mordenite is also shown in Fig. 3. The location of peaks is similar to the zeolite pattern in other synthesized raw materials [34]. So, the result indicates that the zeolite synthesized in this study consists mainly of mordenite. The lack of silica and sodium aluminate peaks in the XRD pattern indicates their removal from cavities in the zeolite.

3.4. SEM analysis

Fig. 4 shows the representative SEM images and EDX studies of the adsorbents. The SEM image of

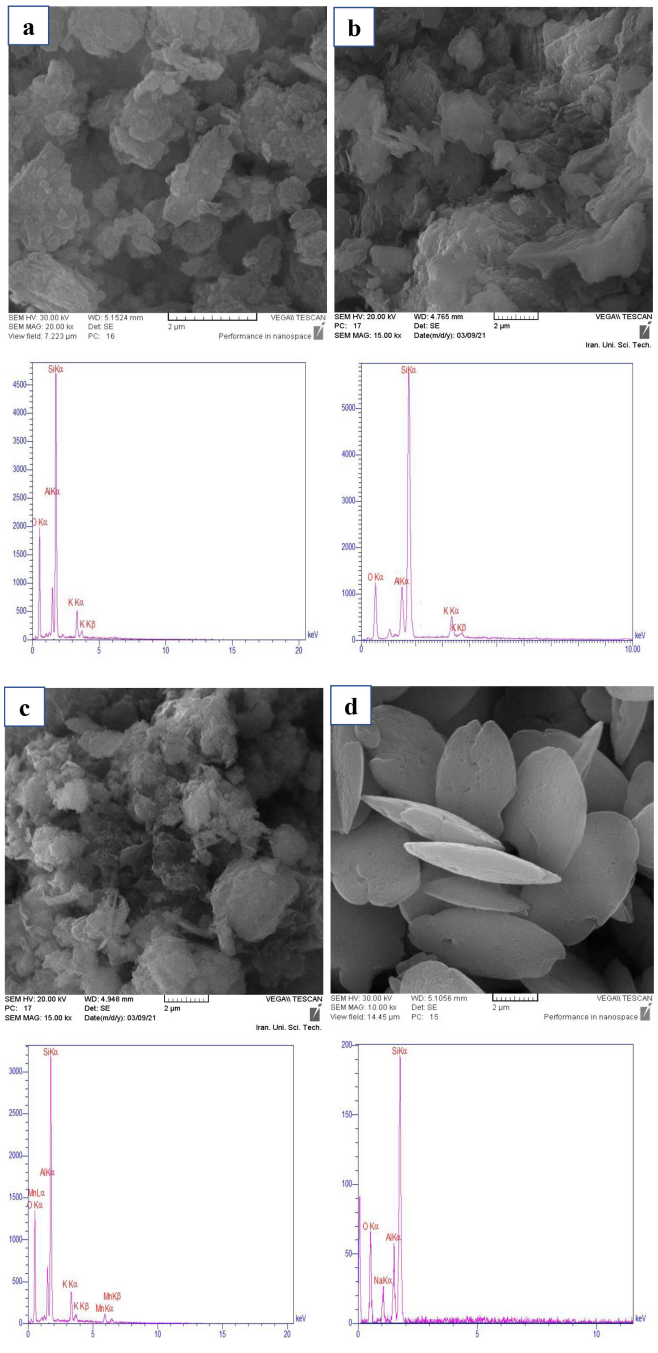

Fig. 4. SEM images and EDX spectra of (a) natural-clino, (b) Us-clino, (c) MnO_2-clino, and (d) synthetic mordenite.

the modified clino, Figs. 4(b) and 4(c), showed that treatment of clinoptilolite with MnO_2 and ultrasound energy does not change the structural appearance of the adsorbent, and there is no change in its morphology compared to the unmodified sample (Fig. 4(a)). As can be seen in the image of the mordenite zeolite in Fig. 4(d), the morphology is similar to lentil. The EDX studies were used to study the chemical composition of adsorbents. The existence peaks in the range of 0.52, 1.04, 3.5, 1.49, and 1.75 keV are attributed to the binding energies of O, Na, K, Al, and Si, respectively [35]. Also, the peaks of Mn observed in EDX spectra (Fig. 4(c)), confirms that synthesis of the MnO_2 phase on the surface of the natural clinoptilolite zeolite was performed.

3.5. Study on phosphate adsorption by adsorbents

The sorption capacity of the adsorbate by porous materials such as zeolites strongly correlates with the surface area, porosity, pore size, and pore volume. The adsorption isotherms of phosphate by the Us-clino, MnO_2-clino, and mordenite zeolites are shown in Fig. 5. As can be seen, the MnO_2-clino and mordenite zeolites have a higher efficiency than the Us-clino in the phosphate adsorption; thus, these adsorbents were selected for investigation of phosphate adsorption.

3.5.1. The effect of contact time

The different contact times in batch adsorption experiments of removal efficiency were investigated at different time values (1.5, 3, 5, 7, 10, 12, 15, 30, 60, and 120 min) to find the optimum adsorption time by MnO_2-clino and mordenite zeolites, see Fig. 6. When the contact time was increased, the removal efficiency also increased because increasing contact time allows enough time for interaction between the phosphate and adsorbents. As can be seen, the adsorption capacity of mordenite improved compared to MnO_2-clino zeolites, and the amount of phosphate adsorbed in all adsorbents increased rapidly, most likely indicating that physical adsorption occurred [36]. The removal efficiency remained stable as contact time increased and achieved the equilibration time. The findings of this study are in agreement with previous batch system literature [37]. The experimental data revealed that the percentage removal of phosphorus was 91.18% at 30 min and 84.14% at 15 min of contact time for mordenite and MnO_2-clino zeolites, respectively. As the experiment shows, the reaction was very close to equilibrium after 120 minutes. So, to save time, 15 and 30 min were considered proper contact times.

3.5.2. The study of adsorbent dosage on phosphate adsorption

The influence of adsorbent dosage at 0.0625, 0.0925, 0.125, 0.25, 0.35, and 0.5 g on phosphate removal is displayed in Fig. 7. The experiment showed that when both absorbents increased adsorbent dosage, the phosphate removal increased because the surface area and adsorption sites increased. However, the phosphate removal did not increase when more adsorbent was added. This observation was due to excess adsorbent in the solution, as observed in other studies [37,38]. So, the

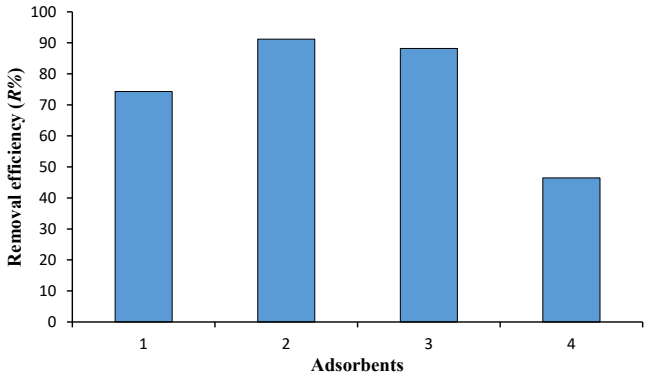

Fig. 5. The removal efficiency (*R%*) of (1) Us-clino, (2) mordenite zeolites, (3) MnO_2-clino, and (4) natural clino (initial concentration of phosphate of 50 $mg.L^{-1}$, adsorbent dose = 5 $g.L^{-1}$, contact time = 30 min, pH = 7, and temperature = 298 K).

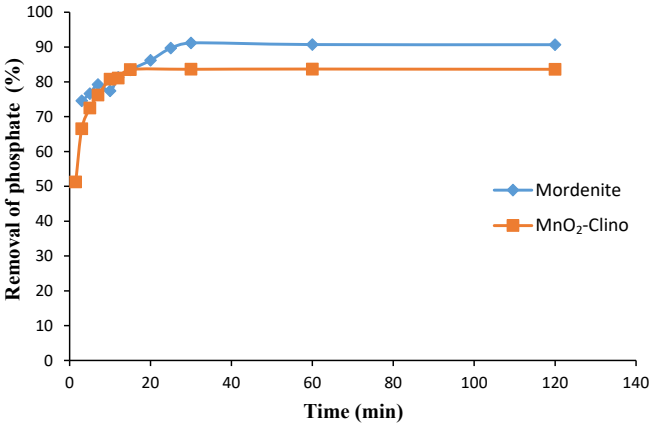

Fig. 6. The effects of contact time on removal efficiency by MnO_2-clino and mordenite zeolites (initial concentration of phosphate of 50 $mg.L^{-1}$, volume = 50 ml, adsorbent dose = 0.25 g, pH = 7, and temperature = 298 K).

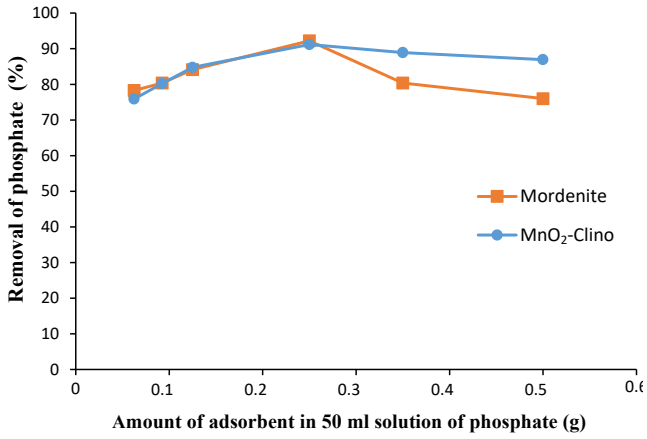

Fig. 7. The effects of adsorbent dosage on removal efficiency by MnO_2-clino and mordenite zeolites (initial concentration of phosphate of 50 $mg.L^{-1}$, volume = 50 ml, contact time = 15 and 30 min for MnO_2-clino and mordenite, respectively, pH = 7, and temperature = 298 K).

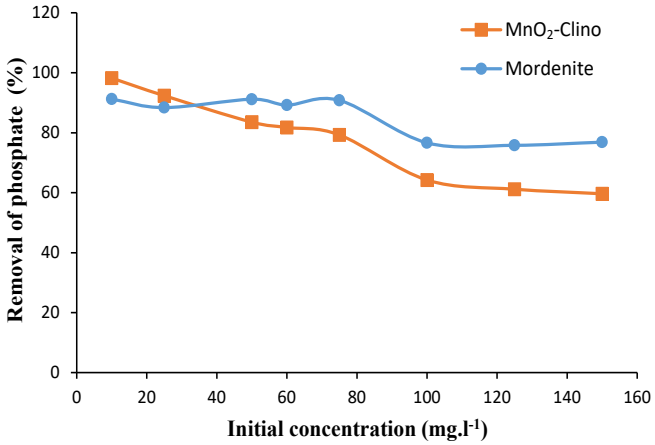

Fig. 8. Effect of initial concentration on the removal phosphate by MnO_2-clino and mordenite zeolites (volume 50 ml, adsorbent dose = 0.25 g, contact time = 15 and 30 min for MnO_2-clino and mordenite, respectively, pH = 7, and temperature = 298 K).

optimum adsorbent dosage was determined to be 0.25 g considering the cost, treatment efficiency, and other factors. This operation factor was used in all subsequent experiments.

3.5.3. Effect of initial phosphate concentration

Fig. 8 shows various initial concentrations on the adsorption of phosphate used to determine the performance of adsorbents. As can be seen, at the low initial concentration, the adsorption rate increased. In other words, as the number of phosphate ions decreases in the low initial concentration, the competition for access to binding sites at the contact surface of the adsorbent is facilitated. So, the adsorption of these ions happens on higher energy sites, while increasing the ion concentration of phosphate causes these sites to be filled, and phosphate ions uptake on lower energy sites. Therefore, the adsorption rate decreases remarkably [31,37].

3.5.4. Studying phosphate adsorption reproducibility by the adsorbents

The percentage of phosphate adsorption, standard deviations, and relative standard deviations (RSD%) for four repeated experiments are given in Table 2. The obtained results show that the efficiency of the adsorbents in removing the phosphate from aqueous samples is good, and they are adsorbed more than 80% by the MnO_2-clino and synthetic mordenite. Furthermore, this process is reproducible with an RSD% of 1.35 and 1.05 for MnO_2-clino and synthetic mordenite, respectively.

3.6. Isotherm of adsorption

The initial and equilibrium concentration of the phosphate are essential parameters to explain the relationship between the adsorbed phosphate concentration and the concentration of the solution at equilibrium in isotherm models. In order to describe the adsorption characteristics, the Langmuir and Freundlich models were studied for the removal of phosphate ions of adsorbents. The monolayer adsorption on an energetically uniform surface is expressed by the Langmuir model. Also, there is no interaction between the adsorbed molecules. So, no more absorption occurs. The multi-layer adsorption is explained by the Freundlich isotherm.

The equations of Langmuir and Freundlich isotherm models are expressed as follows:

$$C_e / q_e = (1/q_m)\, C_e + (1/q_m .b) \quad (4)$$

$$\ln q_e = (1/n) \ln C_e + \ln K_f \quad (5)$$

Table 2. Reproducibility Studies.

Adsorbents	Number of experiments				X ± SD	RSD (%)
	1	2	3	4		
MnO_2-clino	83.62	82.22	84.82	82.9	83.39 ± 1.36	1.35
Synthetic mordenite	91.18	89.8	92.2	90.89	90.94 ± 0.96	1.05

where C_e is the equilibrium concentration in the solution, q_e (mg.g^{-1}) is the phosphate adsorption capacity at equilibrium concentration, and b and q_m are Langmuir constants related to the energy of adsorption and adsorption capacity, respectively. The above parameters were computed from the intercept and linear gradient of graphs of C_e/q_e and C_e (Fig. 9) [39]. Also, the values of the Freundlich constant (K_f) and $1/n$ are obtained from the slope and the intercept of the plot of $\ln q_e$ vs. $\ln C_e$ (Fig. 9). The values of the isotherm parameters of Freundlich and Langmuir models, as well as the correlation coefficients for the adsorbents, are listed in Table 3. The Freundlich and Langmuir equation fitted the experiments because the correlation coefficients of Freundlich and Langmuir (R^2) were 0.99 and 0.91 for synthetic MnO_2-clino and mordenite, respectively.

Table 3. Isotherm parameters for adsorption of phosphate on synthetic mordenite and MnO_2-clino.

Adsorbents	Langmuir isotherm			Freundlich isotherm		
	b (L.mg^{-1})	q_m (mg.g^{-1})	R^2	K_f (L.g^{-1})	n (L.mg^{-1})	R^2
MnO_2-clino	0.1346	18.14	0.96	3.80	2.69	0.99
Synthetic mordenite	0.09	26.95	0.91	2.68	1.60	0.89

$$\ln (q_e - q_t) = \ln (q_e) - (K_1.t) \quad (6)$$

$$t / q_t = (1/(K_2.q_e^{t})) + (t / q_e) \quad (7)$$

$$q_t = K_3.t^{0.5} + C \quad (8)$$

where the phosphate adsorption capacity at equilibrium concentration (mg.g^{-1}) is shown with q_e, the amount of phosphate adsorbed at time t (mg.g^{-1}) is shown with q_t, and the adsorption time (min) is shown with t. The K_1, K_2, and K_3 are represented for the pseudo-first-order rate constant adsorption (L.min^{-1}), the pseudo-second-order rate constant adsorption (g.mg^{-1}.min^{-1}), and the particle diffusion rate constant adsorption (mg.g^{-1}.min$^{-0.5}$), respectively. Also, C (mg.g^{-1}) is the intercept related to the thickness of the boundary layer [40,41]. Fig. 10 shows the parameters for the three adsorption kinetic models as well as the correlation coefficients (R^2) for adsorbents. The results of experiments carried out at 298 K are summarized in Table 4. The table reveals

3.7. The study of kinetics

The batch kinetic adsorption results are helpful in designing adsorption systems and evaluating adsorption efficiency. Pseudo first-order, pseudo second-order, and particle diffusion kinetic models have been used to determine the adsorption mechanism of phosphate removal in optimal experimental conditions. The kinetic equations of pseudo-first-order, pseudo-second-order, and intra particle diffusion or particle diffusion models can be shown as Eqs. (6), (7), and (8) respectively.

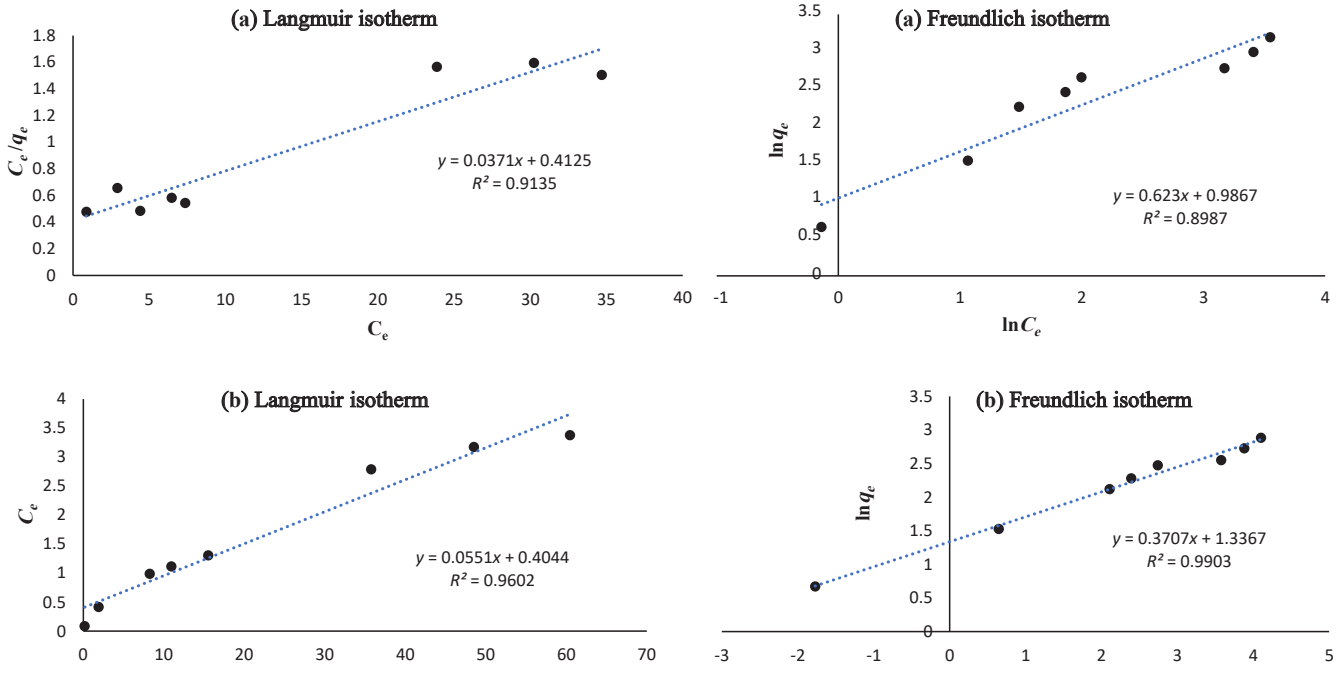

Fig. 9. Linear Langmuir and Freundlich isotherms of phosphate adsorption onto (a) synthetic mordenite and (b) MnO_2-clino.

that the pseudo-second-order kinetic model was better fitted for MnO_2-clino and mordenite zeolites because the amount of R^2 is more than the models.

3.8. The comparison of the adsorption

The adsorption capacities of various adsorbents under different experimental conditions are presented in Table 5. The adsorption capacities of MnO_2-clino and mordenite zeolites used in this study were further compared with that of other adsorbents. Results showed the sorption capacity of MnO_2-clino and mordenite zeolites are adequate for the adsorption of phosphate from an aqueous solution. The high sorption capacity of MnO_2-clino and mordenite zeolites are attributed to more significant specific surface area and surface complexation [42,43].

Table 5. Comparison of maximum adsorption capacity of prepared adsorbents for phosphate adsorption compared with other adsorbents reported in the literature.

Adsorbent	Adsorption capacity ($mg.g^{-1}$)	Reference
$MgCl_2$-biochar	16.09	[44]
BS600	11.45	[45]
La-modified bentonite	14	[46]
La-doped vesuvianite	6.7	[47]
La-impregnated zeolite	7.45	[48]
La-incorporated porous zeolite	17.2	[49]
Synthetic mordenite	23.06	This work
MnO_2-Clino	17.9	This work

4. Conclusions

In summary, the Us-clino, MnO_2-clino, and mordenite zeolites were successfully modified by ultrasound energy, manganese dioxide, and synthesized under solvothermal conditions, respectively. These adsorbents were analyzed and characterized by XRD, SEM, EDXA, FT-IR, and BET techniques. The optimum conditions for removing phosphate using MnO_2-clino and mordenite zeolites were determined at initial concentrations of 150 $mg.L^{-1}$, with 0.25 g of adsorbent, and a contact time of 15 and 30 min, respectively. The maximum adsorption capacity for MnO_2-clino and mordenite zeolites in optimum conditions for phosphate were 17.9 and 23.06 $mg.g^{-1}$, respectively. The study results indicate that the sorption capacity of mordenite is higher than MnO_2-clino because the surface area of mordenite is larger than MnO_2-clino. In addition, the

Table 4. Kinetic parameters for adsorption of phosphate on synthetic mordenite and MnO_2-clino.

Adsorbents	Pseudo-first-order			Pseudo-second-order			Intra-particle diffusion		
	K_1 ($L.min^{-1}$)	q_e ($mg.g^{-1}$)	R^2	K_2 ($g.mg^{-1}.min^{-1}$)	q_e ($mg.g^{-1}$)	R^2	K_2 ($mg.g^{-1}.min^{-0.5}$)	C	R^2
MnO_2-clino	0.005	44.43	0.8	0.0127	8.85	0.99	1.24	4.12	0.89
Synthetic mordenite	0.101	2.79	0.87	0.087	9.2	0.99	0.44	6.61	0.93

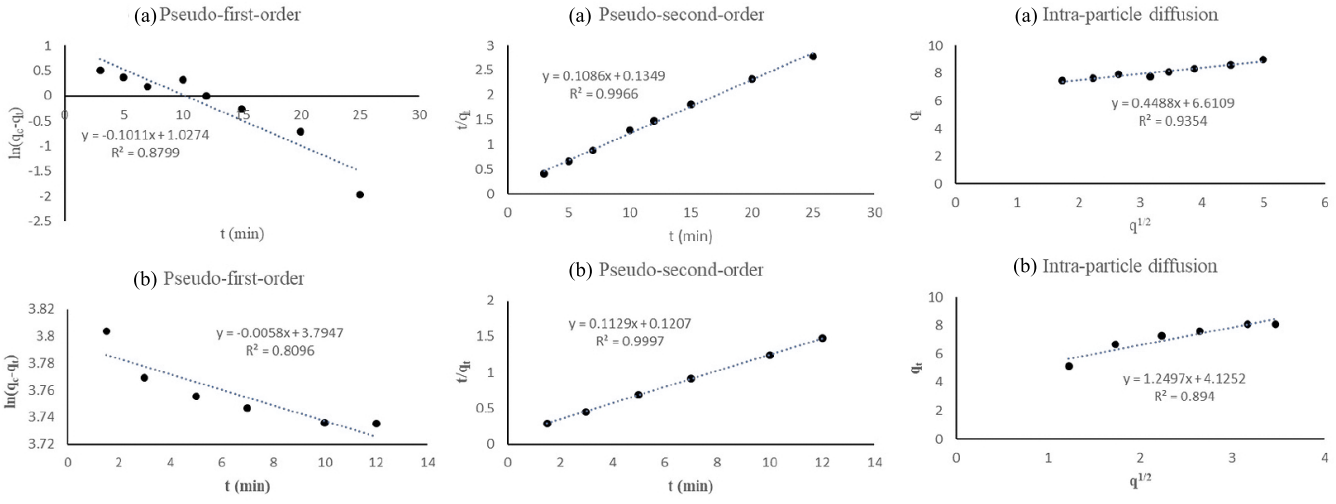

Fig. 10. The pseudo-first-order, pseudo-second-order, and Intra-particle diffusion kinetics curves of phosphate adsorption onto (a) synthetic mordenite and (b) MnO_2-clino.

prepared adsorbents are low cost, non-toxic, and have the potential for phosphate adsorption from aqueous media. The Langmuir and Freundlich's models were used to determine the adsorption isotherms, and the Freundlich and Langmuir equations fitted the synthetic mordenite and MnO_2-clino, respectively. The kinetic analyses indicated that the adsorption process followed pseudo-second-order kinetics.

Acknowledgment

The authors would like to thank the Research Council of the Iran University of Science and Technology (Tehran) for their financial support of this study.

References

[1] A.K. Sethi, V.K. Dwivedi, Exergy analysis of double slope active solar still under forced circulation mode, Desalin. Water Treat. 51 (2013) 7394-7400.

[2] O.M.L. Alharbi, A.A. Basheer, R.A. Khattab, I. Ali, Health and environmental effects of persistent organic pollutants, J. Mol. Liq. 263 (2018) 442-453.

[3] S. Yang, Y. Zhao, R. Chen, C. Feng, Z. Zhang, Z. Lei, *et al.*, A novel tablet porous material developed as adsorbent for phosphate removal and recycling, J. Colloid Interf. Sci. J. 396 (2013) 197-204.

[4] Y. Huang, C. Song, L. Li, Y. Zhou, The mechanism and performance of zeolites for ammonia removal in the zeolite packed electrolysis reactor, Electrochemistry, 82 (2014) 557-560.

[5] T.C. Daniel, A.N. Sharpley, J.L. Lemunyon, Agricultural phosphorus and eutrophication: A symposium overview, J. Environ. Qual. 27 (1998) 251-257.

[6] M. El Wali, S.R. Golroudbary, A. Kraslawski, Impact of recycling improvement on the life cycle of phosphorus, Chin. J. Chem. Eng. 27 (2019) 1219-1229.

[7] R. Li, J.J. Wang, B. Zhou, M.K. Awasthi, A. Ali, Z. Zhang, *et al.*, Recovery of phosphate from aqueous solution by magnesium oxide decorated magnetic biochar and its potential as phosphate-based fertilizer substitute, Bioresource Technol. 215 (2016) 209-214.

[8] D.W. Schindler, The dilemma of controlling cultural eutrophication of lakes, P. Roy. Soc. B-Biol. Sci. 279 (2012) 4322-4333.

[9] P.H. Hsu, Precipitation of phosphate from solution using aluminum salt, Water Res. 9 (1975) 1155-1161.

[10] H.S. Altundoğan, F. Tümen, Removal of phosphates from aqueous solutions by using bauxite. I: Effect of pH on the adsorption of various phosphates, J. Chem. Technol. Biot. 77 (2002) 77-85.

[11] Y. Chen, Y.-S. Chen, Q. Xu, Q. Zhou, G. Gu, Comparison between acclimated and unacclimated biomass affecting anaerobic–aerobic transformations in the biological removal of phosphorus, Process Biochem. 40 (2005) 723-732.

[12] D. Mulkerrins, A.D.W. Dobson, E. Colleran, Parameters affecting biological phosphate removal from wastewaters, Environ. Int. 30 (2004) 249-259.

[13] Y. Li, C. Liu, Z. Luan, X. Peng, C. Zhu, Z. Chen, *et al.*, Phosphate removal from aqueous solutions using raw and activated red mud and fly ash, J. Hazard. Mater. 137 (2006) 374-383.

[14] I. Ali, V.K. Gupta, Advances in water treatment by adsorption technology, Nat. Protoc. 1 (2006) 2661-2667.

[15] S. Salehi, S. Mandegarzad, M. Anbia, Preparation and characterization of metal organic framework-derived nanoporous carbons for highly efficient removal of vanadium from aqueous solution, J. Alloy. Compd. 812 (2020) 152051.

[16] Z. Jin, X. Wang, X. Cui, Synthesis and morphological investigation of ordered SBA-15-type mesoporous silica with an amphiphilic triblock copolymer template under various conditions, Colloid. Surface. A, 316 (2008) 27-36.

[17] T. Sonoda, T. Maruo, Y. Yamasaki, N. Tsunoji, Y. Takamitsu, M. Sadakane, *et al.*, Synthesis of high-silica AEI zeolites with enhanced thermal stability by hydrothermal conversion of FAU zeolites, and their activity in the selective catalytic reduction of NOx with NH_3, J. Mater. Chem. A, 3 (2015) 857-865.

[18] T. Sano, S. Wakabayashi, Y. Oumi, T. Uozumi, Synthesis of large mordenite crystals in the presence of aliphatic alcohol, Micropor. Mesopor. Mater. 46 (2001) 67-74.

[19] T.C. Keller, S. Isabettini, D. Verboekend, E.G. Rodrigues, J. Pérez-Ramírez, Hierarchical high-silica zeolites as superior base catalysts, Chem. Sci. 5 (2014) 677-684.

[20] Y.-P. Zhao, T.-Y. Gao, S.-Y. Jiang, D.-W. Cao, Ammonium removal by modified zeolite from municipal wastewater, J. Environ. Sci.-China, 16 (2004) 1001-1004.

[21] Y. Watanabe, H. Yamada, J. Tanaka, Y. Moriyoshi, Hydrothermal modification of natural zeolites to improve uptake of ammonium ions, J. Chem. Technol. Biot. 80 (2005) 376-380.

[22] Z. Liang, J. Ni, Improving the ammonium ion uptake onto natural zeolite by using an integrated modification process, J. Hazard. Mater. 166 (2009) 52-60.

[23] L. Lei, X. Li, X. Zhang, Ammonium removal from aqueous solutions using microwave-treated natural Chinese zeolite, Sep. Purif. Technol. 58 (2008) 359-366.

[24] A.W. Chester, E.G. Derouane, Zeolite characterization and catalysis, Springer, 2009.

[25] P. Benito, F.M. Labajos, J. Rocha, V. Rives, Influence of microwave radiation on the textural properties of layered double hydroxides, Micropor. Mesopor. Mater. 94 (2006) 148-158.

[26] J.A. Rivera, G. Fetter, P. Bosch, Microwave power effect on hydrotalcite synthesis, Micropor. Mesopor. Mater. 89 (2006) 306-314.

[27] O. Bergadà, I. Vicente, P. Salagre, Y. Cesteros, F. Medina, J.E. Sueiras, Microwave effect during aging on the porosity and basic properties of hydrotalcites, Micropor. Mesopor. Mater. 101 (2007) 363-373.

[28] I. Vicente, P. Salagre, Y. Cesteros, F. Guirado, F. Medina, J.E. Sueiras, Fast microwave synthesis of hectorite, Appl. Clay Sci. 43 (2009) 103-107.

[29] R.M. Barrer, 435. Syntheses and reactions of mordenite, J. Chem. Soc. (1948) 2158-2163.

[30] J. Behin, H. Kazemian, S. Rohani, Sonochemical synthesis of zeolite NaP from clinoptilolite, Ultrason. Sonochem. 28 (2016) 400-408.

[31] F. Yazdi, M. Anbia, S. Salehi, Characterization of functionalized chitosan-clinoptilolite nanocomposites for nitrate removal from aqueous media, Int. J. Biol. Macromol. 130 (2019) 545-555.

[32] H. Zabihi-Mobarakeh, A. Nezamzadeh-Ejhieh, Application of supported TiO_2 onto Iranian clinoptilolite nanoparticles in the photodegradation of mixture of aniline and 2, 4-dinitroaniline aqueous solution, J. Ind. Eng. Chem. 26 (2015) 315-321.

[33] Y. Dong, Y. Xue, W. Gu, Z. Yang, G. Xu, MnO_2 nanowires/CNTs composites as efficient non-precious metal catalyst for oxygen reduction reaction, J. Electroanal. Chem. 837 (2019) 55-59.

[34] Y. Wang, Y. Kmiya, T. Okuhara, Removal of low-concentration ammonia in water by ion-exchange using Na-mordenite, Water Res. 41 (2007) 269-276.

[35] S. Salehi, M. Hosseinifard, Highly efficient removal of phosphate by lanthanum modified nanochitosan-hierarchical ZSM-5 zeolite nano-composite: characteristics and mechanism, Cellulose, 27 (2020) 4637-4664.

[36] D. Bhardwaj, M. Sharma, P. Sharma, R. Tomar, Synthesis and surfactant modification of clinoptilolite and montmorillonite for the removal of nitrate and preparation of slow release nitrogen fertilizer, J. Hazard. Mater. 227-228 (2012) 292-300.

[37] T.-H. Pham, K.-M. Lee, M.S. Kim, J. Seo, C. Lee, La-modified ZSM-5 zeolite beads for enhancement in removal and recovery of phosphate, Micropor. Mesopor. Mater. 279 (2019) 37-44.

[38] M. Zhang, H. Zhang, D. Xu, L. Han, J. Zhang, L. Zhang, *et al*., Removal of phosphate from aqueous solution using zeolite synthesized from fly ash by alkaline fusion followed by hydrothermal treatment, Sep. Sci. Technol. 46 (2011) 2260-2274.

[39] R.F. Spalding, M.E. Exner, Occurrence of Nitrate in Groundwater - A review, J. Environ. Qual. 22 (1993) 392-402.

[40] D.S. Powlson, T.M. Addiscott, N. Benjamin, K.G. Cassman, T.M. de Kok, H. van Grinsven, *et al*., When Does Nitrate Become a Risk for Humans?, J. Environ. Qual. 37 (2008) 291-297.

[41] L. Knobeloch, B. Salna, A. Hogan, J. Postle, H. Anderson, Blue babies and nitrate-contaminated well water, Environ. Health Persp. 108 (2000) 675-678.

[42] K. Wu, Y. Li, T. Liu, N. Zhang, M. Wang, S. Yang, *et al.*, Evaluation of the adsorption of ammonium-nitrogen and phosphate on a granular composite adsorbent derived from zeolite, Environ. Sci. Pollut. R. 26 (2019) 17632-17643.

[43] J.-R. Li, F.-K. Wang, H. Xiao, L. Xu, M.-L. Fu, Layered chalcogenide modified by Lanthanum, calcium and magnesium for the removal of phosphate from water, Colloid. Surface. A, 560 (2019) 306-314.

[44] K.-W. Jung, K.-H. Ahn, Fabrication of porosity-enhanced MgO/biochar for removal of phosphate from aqueous solution: Application of a novel combined electrochemical modification method, Bioresource Technol. 200 (2016) 1029-1032.

[45] J.-R. Li, L. Zhu, J. Tang, K. Qin, G. Li, T. Wang, Sequestration of naturally abundant seawater calcium and magnesium to enhance the adsorption capacity of bentonite toward environmental phosphate, Rsc Adv.

6 (2016) 23252-23259.

[46] V. Kuroki, G.E. Bosco, P.S. Fadini, A.A. Mozeto, A.R. Cestari, W.A. Carvalho, Use of a La(III)-modified bentonite for effective phosphate removal from aqueous media, J. Hazard. Mater. 274 (2014) 124-131.

[47] H. Li, J. Ru, W. Yin, X. Liu, J. Wang, W. Zhang, Removal of phosphate from polluted water by lanthanum doped vesuvianite, J. Hazard. Mater. 168 (2009) 326-330.

[48] Y. He, H. Lin, Y. Dong, Q. Liu, L. Wang, Simultaneous removal of ammonium and phosphate by alkaline-activated and lanthanum-impregnated zeolite, Chemosphere, 164 (2016) 387-395.

[49] Y. He, H. Lin, Y. Dong, L. Wang, Preferable adsorption of phosphate using lanthanum-incorporated porous zeolite: Characteristics and mechanism, Appl. Surf. Sci. 426 (2017) 995-1004.